Available online at www.sciencedirect.com

SciVerse ScienceDirect

Ceramics International 38 (2012) 4861–4866

CERAMICS INTERNATIONAL

www.elsevier.com/locate/ceramint

Using modified Pechini method to synthesize α-Al_2O_3 nanoparticles of high surface area

T. Zaki [a,*], Khalid I. Kabel [b], H. Hassan [a]

[a] Catalysis Department, Refining Division, Egyptian Petroleum Research Institute, Nasr City, P.B. 11727, Cairo, Egypt
[b] Additives Department, Applications Division, Egyptian Petroleum Research Institute, Nasr City, P.B. 11727, Cairo, Egypt

Received 14 January 2012; received in revised form 25 February 2012; accepted 26 February 2012
Available online 6 March 2012

Abstract

A modified Pechini method for the preparation of a high surface area α-alumina is proposed. The synthesis of these nanoparticles was carried out using a polymer as a chelating agent. The polymer was prepared from citric acid and acrylic acid by the melt blending method. The resulting α-alumina (98.16%) after calcination at 900 °C consisted of cylindrical nanoparticles of 100–200 nm in length and <25 nm in diameter with a relatively high surface area (18 $m^2 g^{-1}$).

Keywords: α-Alumina; Pechini method; Citric acid; Acrylic acid; Nanoparticles

1. Introduction

In recent years, metal nanoparticles provide tunable catalytic properties due to the presence of a large number of surface atoms [1]. Corundum (α-Al_2O_3) has significant importance in the field of catalytic applications because it exists in a thermodynamically stable phase at standard pressure and temperature conditions [2,3]. However, its very low surface area represents a serious drawback.

The coupling of the polymer and nanoparticle worlds holds great promise. The polymeric materials can be tailor-modified at the nanoparticle surface to display a range of specific functional groups [4–6].

The Pechini method belongs to the sol–gel category of fabrication methods. In this method, an α-hydroxycarboxylic-containing compound forms a polybasic acid chelate with metal cations; which successively polymerize with a polyhydroxy alcohol [7]. After calcination process, nanometer-sized powders are achieved. When compared to other sol-gel methods, the Pechini method has better compositional homogeneity, lower toxicity and lower cost [8,9].

Different researches have focused on synthesizing α-Al_2O_3 of limited phase mass fraction at high calcination temperatures (1100 °C) to get a relatively high surface area product [10,11]. Recently, Mahapatra et al. prepared α-Al_2O_3 with high surface area using the electrospinning method [12]. In previous, we have succeeded in getting α-alumina (98.95% mass fraction and ~8 $m^2 g^{-1}$ surface area) at relatively low calcination temperature (925 °C), based on the synthesis parameters of Pechini method [13].

In the present study, a modified water-based Pechini method was adopted to prepare α-alumina nanoparticles that are highly crystalline and have a higher specific surface area (18–66 $m^2 g^{-1}$) at the relatively lower calcination temperature of 900 °C than the previous prepared α-alumina samples [13].

2. Experimental

2.1. Polymer preparation

In a three-neck round-bottom flask fitted with a thermometer and condenser, 0.12 mole of anhydrous citric acid (CA, Sigma–Aldrich, assay ≥99.5%) was mixed with 0.1 mole of acrylic acid (AA, Sigma–Aldrich, assay ≥99.0%) in the presence of 0.1% hydroquinone (HQ, Merck, assay ≥99.0%). The blend temperature was increased gradually to 120–170 °C. The esterification occurred at about 120 °C, and the polymerization

* Corresponding author. Fax: +20 2 22747433.
E-mail address: tamerzakisharara@yahoo.com (T. Zaki).

0272-8842/$36.00
doi:10.1016/j.ceramint.2012.02.076

was carried out at higher temperatures to obtain a high viscosity polymer with a white yellowish color. The synthesis of the polymer was carried out according to the following equation:

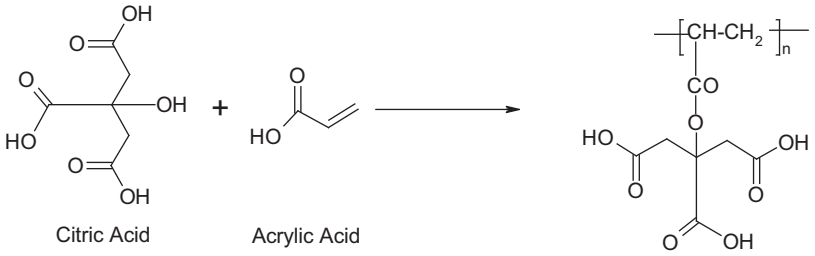

The acidity of the prepared viscous polymer was measured via titration against a solution of 0.05 N NaOH. One gram of the prepared viscous polymer was equivalent to 28.16 μmole NaOH. The FT-IR spectrum of the prepared viscous polymer (Fig. 1) indicates the presence of a C=O ester group at 1740 cm^{-1}.

The average molecular weight of the prepared polymer was measured by gel permeation chromatography as previously mentioned [13]. The determined average molecular weight of the polymer (1247 g/mol) was higher than the theoretically calculated weight (282.2 g/mol). The polydispersity index was equal to 1.2.

2.2. Alumina preparation

Five different alumina powders were prepared using the polymerizing–chelating synthesis process. For all of the prepared samples, 10 g of the previously made viscous polymer was heated to 80 °C with stirring. The experimental details of the polymerizing–chelating, drying and successively pyrolysis processes are described previously [13].

The required volume of an aluminum nitrate nonahydrate (Sigma–Aldrich, assay ≥98.0%) solution with desired concentration was added to the polyester. Stirring was continued for another hour. The solutions were then slowly heated to 140 °C and maintained at this temperature until removal of water was almost complete (2.5 h). The clear gels obtained from this process were transferred to an electrical furnace and dried at 150 °C overnight, yielding solid resins of high porosity. The resulting resins were ground in an agate mortar and subjected to a pyrolysis process at 450 °C (heating rate 5 °C/min) for 4 h in glazed alumina crucibles. Finally, the pyrolysis product was subjected to a calcination process at 900 °C (heating rate 5 °C/min) for 4 h in the presence of purified air.

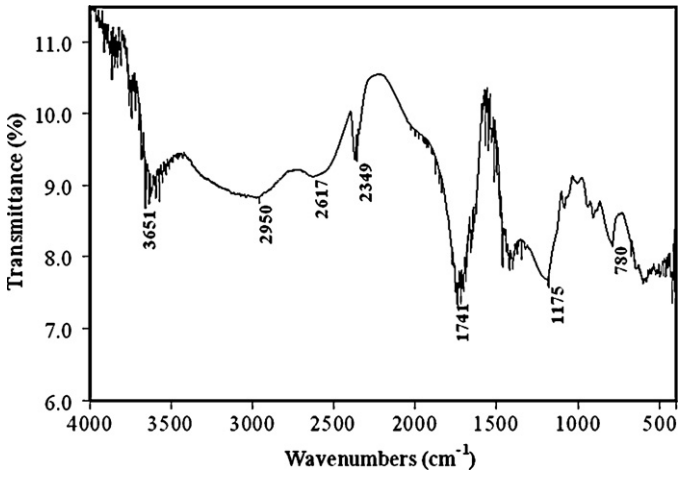

Fig. 1. FT-IR spectrum of the as-prepared polymer.

The prepared materials are listed in Table 1 and named according to their synthesis differences. Alumina samples were prepared using a variety of CA-to-Al^{3+} molar ratios, as well as different concentrations of the aluminum nitrate solution, at a constant CA-to-AA molar ratio. The samples were named AlR_C–R_A, where R_C is the CA:Al^{3+} ratio and R_A is the aluminum precursor concentration.

2.3. Analytical methods

Differential thermal analyses coupled with thermogravimetric analysis (TGA) of the solid resins were recorded on a SDT Q600 Simultaneous DSC/TGA Analyzer manufactured by TA Instruments, Inc. (USA). The run was carried out in air at a heating rate of 10 °C/min. The crystalline structure of the prepared powders was analyzed by X-ray diffractometry (X-Pert PRO, PAN analytical, Netherlands) using CuKα radiation in the angular region of $2\theta = 4–70°$. For phase identification purposes, automatic JCPDS library search and match were used. The mass fraction of α-alumina in the calcined products was estimated with respect to the relative intensity of the (2 0 0) reflection of θ-alumina. Identification of the constituents of the optimum α-alumina sample was carried out using PAN analytical Axios advanced X-ray fluorescence. The surface area of different samples of the prepared α-alumina was determined from the adsorption of nitrogen gas at liquid nitrogen temperature (–195.8 °C) using NONA3200e (Quantachrome – USA). Prior to such measurements, all samples were perfectly degassed at 150 °C and 10^{-4} Torr overnight. FT-IR spectra (KBr disc method) were recorded on an ATI/Unicam Infinity 961 M instrument. High resolution transmission electron microscopy image (HRTEM) was recorded on a JEOL JEM-2100 electron microscope at 200 kV equipped with EDS (D2-LN2 free silicon drift detector – Oxford X-Max) used for the analysis of chemical composition.

Table 1
Amounts, concentrations and ratios of reactants, % weight loss of dried resins according to TGA, mass fraction of α-alumina, and the BET surface area (S_{BET}) of prepared α-alumina samples.

Material	CA	AA	Al salt solution		$CA:Al^{3+}$	Wt loss	α-Al_2O_3	S_{BET}
	(g)	(mL)	(mole/L)	(mL)	(molar ratio)	(%)	(%)	($m^2\ g^{-1}$)
Al9–19	0.12	0.03	0.19	500	0.09	51.9	98.16	18.19
Al9–9	0.12	0.03	0.09	1000	0.09	51.6	88.18	25.78
Al9–6	0.12	0.03	0.06	1500	0.09	52.7	87.84	29.82
Al13–13	0.12	0.03	0.13	500	0.13	54.6	85.34	33.03
Al21–8	0.12	0.03	0.08	500	0.21	61.7	69.27	65.85

3. Results and discussion

3.1. Thermal analysis (DSC–TGA)

The thermal behavior observed in all samples was typical of that found in other polymerized complex resins. In the TG curves (Fig. 2), a substantial weight loss was observed in the range 400–800 °C, accompanied by a broad significant exothermic peak (Fig. 3), which is resulted from the thermal decomposition of the organic species [14]. The broadening of the exothermic peak increased as the CA/Al^{3+} molar ratio increased (Table 1). Such behavior could be attributed to the increasing of the amount of the unreacted carboxylic groups, which make the decomposition process more complicated and slower.

The transformation of alumina into the alpha phase resulted in the appearance of distinct exothermic peaks in a narrow range of temperatures (870–900 °C; Fig. 3). The Al9–19 sample formed the α-alumina phase at the lowest temperature (872 °C). The DSC curves revealed that the formation temperature of α-alumina increased as the CA/Al^{3+} molar ratio increased (Table 1). Also, the formation temperature of α-alumina increased as the concentration of the aluminum precursor decreased.

3.2. X-ray analysis

The XRD patterns of the calcined samples at 900 °C (Fig. 4) confirm the consistence with the reference XRD pattern of α-Al_2O_3 powder (JCPDS file 42–1468 – Fig. 4f). XRD patterns of the samples showed the presence of monoclinic θ-alumina as a minor phase (JCPDS file 35-0121 – Fig. 4b, d and e respectively).

Table 1 shows that the mass fraction of α-alumina decreased as the concentration of aluminum precursor decreased, and as the CA/Al^{3+} molar ratio increased. The high mass fraction of α-alumina in the Al9–19 sample (98.16%) may be attributed to the low temperature at which the α-alumina phase formed (872 °C – Fig. 3).

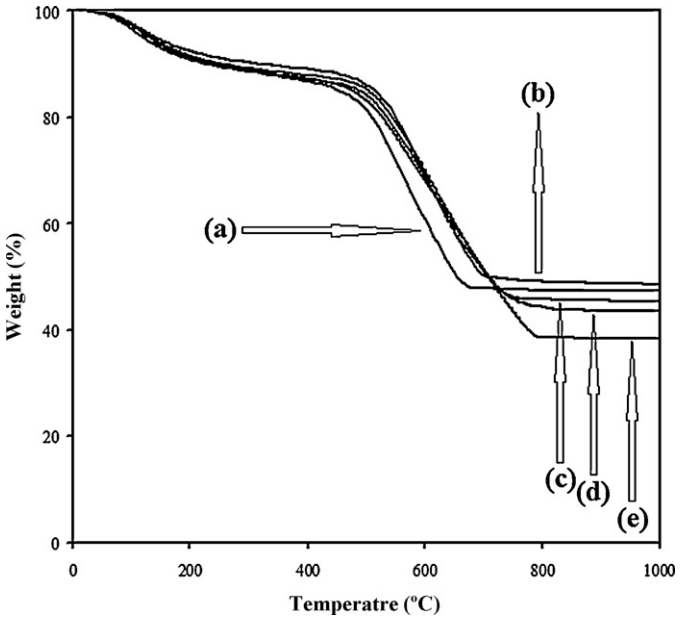

Fig. 2. TGA profiles for resins of (a) Al9–19, (b) Al9–9, (c) Al9–6, (d) Al13–13, and (e) Al21–8 samples.

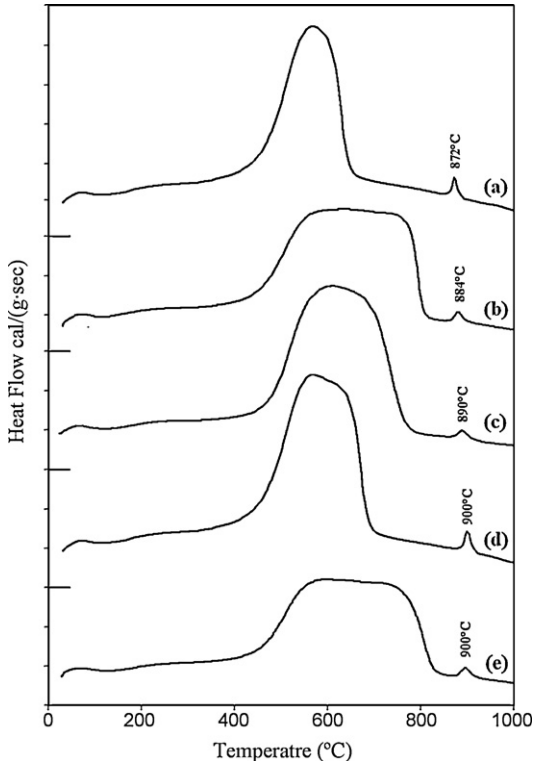

Fig. 3. DSC curves for resins of (a) Al9–19, (b) Al9–9, (c) Al9–6, (d) Al13–13, and (e) Al21–8 samples.

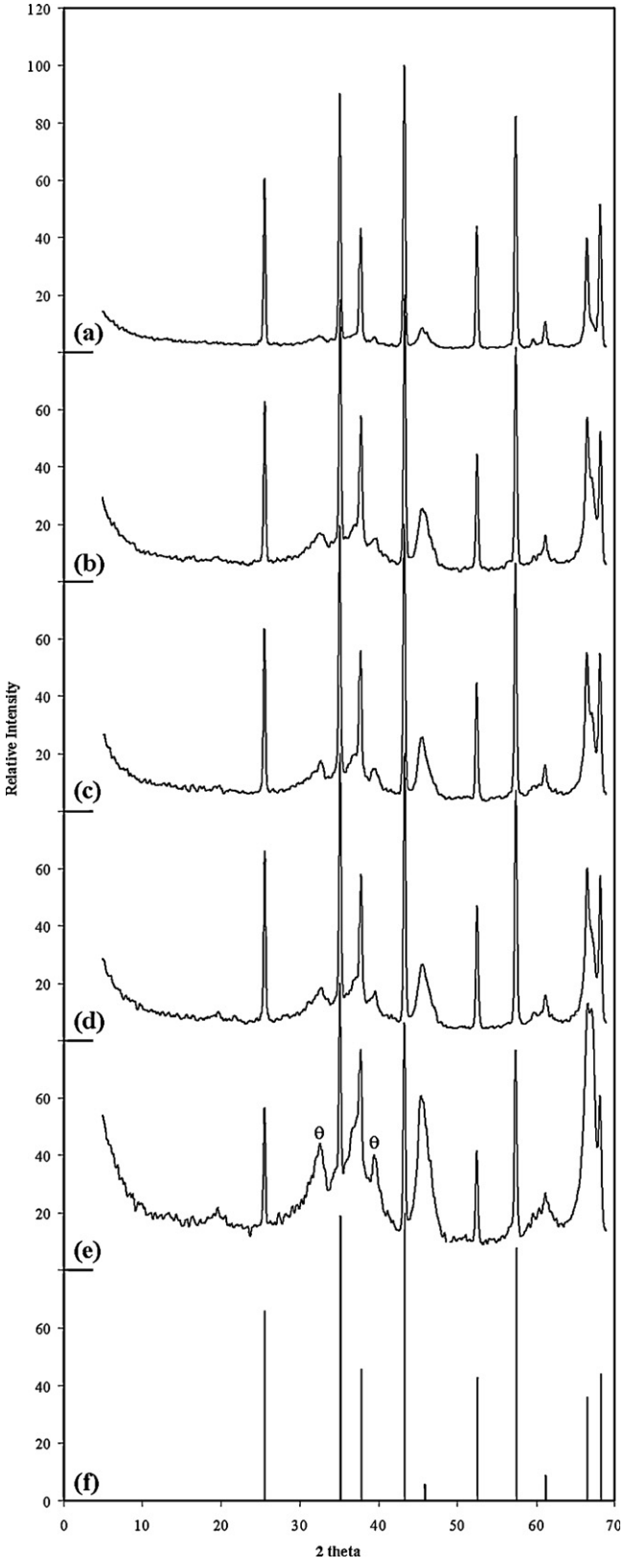

Fig. 4. X-ray diffraction patterns of (a) Al9–19, (b) Al9–9, (c) Al9–6, (d) Al13–13, and (e) Al21–8 samples compared with (f) α-alumina (JCPDS files no. 42-1468).

Table 2
Chemical analysis of Al9–19 sample.

Main constituents	wt%
Na_2O	0.015
MgO	–
Al_2O_3	98.955
SiO_2	–
K_2O	–
P_2O_5	0.016
SO_3	–
CaO	0.020
TiO_2	–
Fe_2O_3	0.021
NiO	0.023
CuO	0.011
ZnO	–
SrO	–
ZrO_2	0.019
Cl	–
L.O.I	0.920

Loss of ignition (L.O.I), as determined by burning 1 g sample at 1000 °C till constant weight.

The chemical analysis of the Al9–19 sample (Table 2) using XRF indicates that: it possesses high alumina content (∼98.96%), traces Na_2O 0.015%, as well as traces percentage of CaO (0.020%), and Fe_2O_3 (0.021%). The ignition loss at 1000 °C was 0.920% could be attributed to releasing of the adsorbed water and/or at the presence of the amorphous carbon impurities that could be detected by CO and CO_2 emission, in addition to the transformation of minor θ-alumina into of α-alumina.

3.3. Nitrogen adsorption-desorption technique

The surface area measurements obtained from nitrogen adsorption–desorption at –195.8 °C are listed in Table 1 (S_{BET}). Results showed a positive proportion between the mass fraction of θ-alumina and the surface area of the materials; whereas the Al21–8 sample showed a very high value for measured surface area (∼66 $m^2\ g^{-1}$).

3.4. Fourier transform infrared spectroscopy (FT-IR)

IR spectrum of Al9–19 (Fig. 5a) presents bands at 609 and 651 cm^{-1} which are characteristics for octahedral AlO_6 stretching modes and at 460 cm^{-1} which due to AlO_6 bending modes [15]. The IR spectrum of Al9–19 (Fig. 5a) and its XRD pattern (Fig. 4a) confirmed the presence of α-Al_2O_3 (octahedron AlO_6 only) as the major phase (∼98%).

The IR spectrum of Al21-8 (Fig. 5b) presents a wide, unresolved pattern extending from 547 cm^{-1} to 875 cm^{-1}, with maximum transmittance around 468 cm^{-1}. This unresolved wide structure is typical of a complex and disordered crystallographic structure, which could be attributed to AlO_4 and AlO_6 stretching modes [15]. The high surface area of the sample causes enlargement in the band that is observed at 3467 cm^{-1}, which results from water deformation vibrations. The IR spectrum (Fig. 5b) and XRD pattern (Fig. 4e) of Al21-8

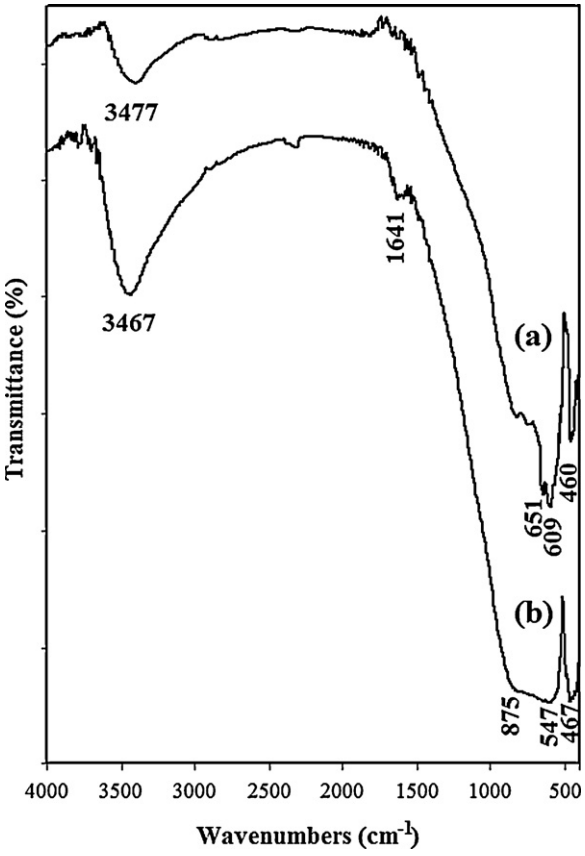

Fig. 5. FT-IR spectrum of (a) Al9–19, and (b) Al21–8 samples.

confirmed the presence of α-Al_2O_3 (octahedron AlO_6 only) in addition to θ-Al_2O_3 (both octahedron AlO_6 and tetrahedron AlO_4).

3.5. TEM and EDX analysis

The EDX spectrum of the Al9–19 sample indicates its high purity (Fig. 6), in agreement with XRF analysis (Table 2). In EDX measurement, caution is needed due to the presence of oxygen in the sample which often showed a low sensitivity that result a non-stoichiometric ratio of Al and O values [16]. The foreign peaks related to copper, carbon and gold (Fig. 6) could be related to the type of the used grid, the amorphous carbon impurities and the fixation nails respectively. The TEM

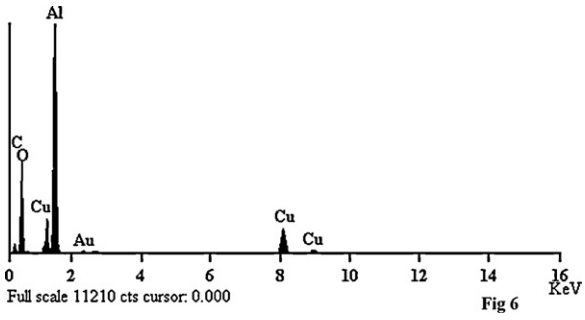

Fig. 6. EDX spectrum of the Al9–19 sample.

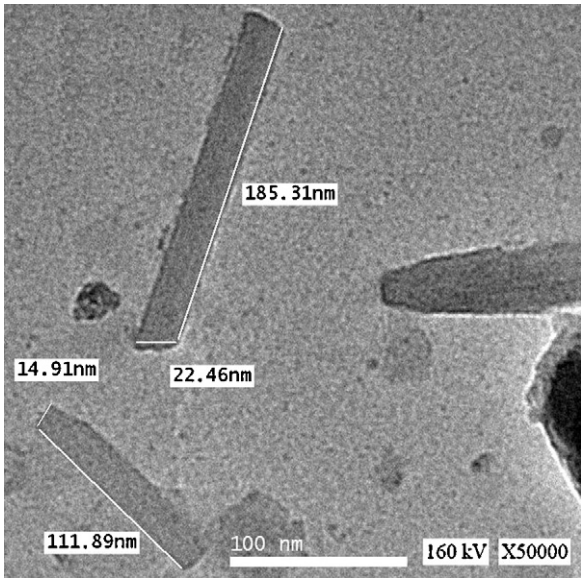

Fig. 7. TEM micrograph of the Al9–19 sample.

micrograph of Al9–19 (Fig. 7) showed that the material is composed of cylindrical particles of 100–200 nm in length and <25 nm diameter.

3.6. Effect of synthesis method on final product

The molecular structure of citric acid contains three carboxylic groups and one hydroxyl group, while the molecule of acrylic acid contains one carboxylic group in addition to the unsaturated terminal. The esterification and polymerization reactions are only possible between the carboxylic group of acrylic acid and the hydroxyl group of citric acid, giving rise to a polymer of long chain structures [14]. It is well known that in a chelation reaction it is important to consider the number of reactive sites in the polymer that are able to bond with metal cations. In this synthesized polymer, the free carboxylic groups of citric acid were the only reactive sites, and these functional groups are likely oriented in different directions around the long hydrocarbon chain to avoid a strain effect.

In the case of alumina nanoparticles prepared with a high CA/Al^{3+} molar ratio, such as the Al21–8 sample, it is likely that the excess free carboxylic groups along the hydrocarbon chain resulted in the formation of a fairly stable complex between citrate and the metal ion due to the strong coordination. Such a structure could slow the removal of the hydrocarbon resin during the calcination process, resulting in formation of α-alumina at higher temperatures.

On the other hand, in the case of a low CA/Al^{3+} molar ratio and a more concentrated aluminum precursor solution, such as the Al9–19 sample, the bonding of a metal ion to the less prevalent, strained free carboxylic groups is therefore assumed to be weaker because of the inability to form stable chelated complexes. Such a structure results in the creation of small agglomerates during the thermal treatment and a decrease in the temperature required for the transformation of other phases of alumina into α-alumina.

It is also important to consider the possibility that the polymer used in this preparation may act as a template that increases the surface area of the resulting α-alumina. Additionally, the decomposition atmosphere may also influence the polymer-containing precursor; thus when the sample is decomposed in nitrogen and the remaining carbon is later thermally removed, the resulting α-alumina had a larger surface area. This effect can be attributed to the remaining carbon which prevents particles from sintering even when heated up to extremely high temperatures. Decomposition in air rather than nitrogen removes the carbon, leaving empty pores in the material [2].

4. Conclusion

A series of highly crystalline α-Al_2O_3 samples with high surface area were prepared using a modified Pechini process. The features of the final products were influenced by the CA/Al^{3+} molar ratio and the dilution of the reactant during the polymerization stage. Manipulation of the above-mentioned factors resulted in the transformation of alumina into the α-phase as cylindrical nanoparticles at the low calcination temperature of 900 °C.

References

[1] Y. Takahashi, W. Yukita, M. Chatterjee, T.M. Suzuki, Preparation of highly dispersed gold nanoparticles inside the porous support assisted by amphiphilic vinyl maleate copolymer, React. Funct. Polym. 68 (2008) 1476–1482.
[2] M.M. Martín-Ruiz, L.A. Pérez-Maqueda, T. Cordero, V. Balek, J. Subrt, N. Murafa, J. Pascual-Cosp, High surface area α-alumina preparation by using urban waste, Ceram. Int. 35 (2009) 2111–2117.
[3] M. Kralik, A. Biffis, Catalysis by metal nanoparticles supported on functional organic polymers, J. Mol. Catal. A: Chem. 177 (2001) 113–138.
[4] F. Truica-Marasescu, S. Pham, M.R. Wertheimer, VUV processing of polymers: Surface modification and deposition of organic thin films, Nucl. Instrum. Methods Phys. Res., Sect. B 265 (2007) 31–36.
[5] C. Schmidt, G. Schmidt-Naake, Grafting of 1-vinylimidazole onto pre-irradiated ETFE films, Macromol. Mater. Eng. 292 (2007) 1067–1074.
[6] F. Munoz-Munoz, J.-C. Ruiz, C. Alvarez-Lorenzo, A. Concheiro, E. Bucio, Novel interpenetrating smart polymer networks grafted onto polypropylene by gamma radiation for loading and delivery of vancomycin, Eur. Polym. J. 45 (2009) 1859–1867.
[7] G. He, J.H. Cai, G. Ni, ZnO thin films prepared by a modified water-based Pechini method, Mater. Chem. Phys. 110 (2008) 110–114.
[8] X. Ding, Y. Liu, L. Gao, L. Guo, Synthesis and characterization of doped $LaCrO_3$ perovskite prepared by EDTA–citrate complexing method, J. Alloys Compd. 458 (2008) 346–350.
[9] G.P. da Silva, M. Mack, J. Contiero, Glycerol: A promising and abundant carbon source for industrial microbiology, Biotechnol. Adv. 27 (2009) 30–39.
[10] Y. Sarikaya, T. Alemdaroglu, M. Onal, Determination of the shape, size and porosity of fine α-Al_2O_3 powders prepared by emulsion evaporation, J. Eur. Ceram. Soc. 22 (2002) 305–309.
[11] Y.C. Lee, S.B. Wen, W.L. Liang, C.P. Lin, Nano α-Al_2O_3 powder preparation by calcining an emulsion precursor, J. Am. Ceram. Soc. 90 (2007) 1723–1727.
[12] A. Mahapatra, B.G. Mishra, G. Hota, Synthesis of ultra-fine α-Al_2O_3 fibers via electrospinning method, Ceram. Int. 37 (2011) 2329–2333.
[13] T. Zaki, Khalid I. Kabel, H. Hassan, Preparation of high pure α-Al_2O_3 nanoparticles at low temperatures using Pechini method, Ceram. Int. 38 (2012) 2021–2026.
[14] M.T. Hernández, M. González, Synthesis of resins as alpha-alumina precursors by the Pechini method using microwave and infrared heating, J. Eur. Ceram. Soc. 22 (2002) 2861–2868.
[15] A. Boumaza, L. Favaro, J. Lédion, G. Sattonnay, J.B. Brubach, P. Berthet, A.M. Huntz, P. Roy, R. Tétot, Transition alumina phases induced by heat treatment of boehmite: An X-ray diffraction and infrared spectroscopy study, J. Solid State Chem. 182 (2009) 1171–1176.
[16] C.K. Kumara, W.J. Ng, A. Bandara, R. Weerasooriya, Nanogibbsite: Synthesis and characterization, J. Colloid Interface Sci. 352 (2010) 252–258.